k_T effects in direct-photon production

L. Apanasevich, C. Balázs, C. Bromberg, J. Huston, A. Maul, and W. K. Tung
Department of Physics and Astronomy, Michigan State University, East Lansing, Michigan 48824

S. Kuhlmann
High Energy Physics Divison, Argonne National Laboratory, Argonne, Illinois 60439

J. Owens
High Energy Physics, Florida State University, Tallahassee, Florida 32306

M. Begel, T. Ferbel, G. Ginther, P. Slattery, and M. Zieliński
Department of Physics and Astronomy, University of Rochester, Rochester, New York 14627
(Received 29 September 1998; published 18 February 1999)

We discuss the phenomenology of initial-state parton-k_T broadening in direct-photon production and related processes in hadron collisions. After a brief summary of the theoretical basis for a Gaussian-smearing approach, we present a systematic study of recent results on fixed-target and collider direct-photon production, using complementary data on diphoton and pion production that provide empirical guidance on the required amount of k_T broadening. This approach provides a consistent description of the observed pattern of deviation of next-to-leading order QCD calculations relative to the direct-photon data, and accounts for the shape and normalization difference between fixed-order perturbative calculations and the data. We also discuss the uncertainties in this phenomenological approach, the implications of these results on the extraction of the gluon distribution of the nucleon, and the comparison of our findings to recent related work.
[S0556-2821(99)03805-9]

PACS number(s): 12.38.Qk, 13.85.Ni, 13.85.Qk

INTRODUCTION

Direct-photon production has long been viewed as an ideal process for measuring the gluon distribution in the proton [1]. The quark-gluon Compton scattering subprocess ($gq \rightarrow \gamma q$) dominates γ production in all kinematic regions of pp scattering, as well as for low to moderate values of parton-momentum fraction, x, in $\overline{p}p$ scattering; the cross sections have been calculated to next-to-leading order (NLO) [2]. The gluon distribution in the proton is relatively well constrained at small x ($x<0.1$) by deep-inelastic scattering (DIS) and Drell-Yan (DY) data, but less so at larger x [3]. Consequently, direct-photon data from fixed-target experiments that have been incorporated in several modern global parton distribution function analyses can, in principle, provide an important constraint on the gluon content at moderate to large x [4–7].

However, a pattern of deviations between the measured direct-photon cross sections and NLO calculations has been observed [8]. The discrepancy is particularly striking in the recently published higher-statistics data from E706 experiment [9]. E706 observed large deviations between NLO calculations and data, for both direct-photon and π^0 inclusive cross sections. The final direct-photon results from UA6 [10] also exhibit evidence of similar, although smaller, discrepancies. The suspected origin of the disagreements is from effects of initial-state soft-gluon radiation. Such radiation generates transverse components of initial-state parton momenta, referred to in this discussion as k_T. To be precise, as in [9], k_T denotes the magnitude of the effective transverse momentum vector, $\vec{k}_T$, of each of the two colliding partons.

Evidence of significant k_T has long been observed in measurements of dimuon, diphoton, and dijet pairs. A collection of measurements of the average transverse momentum of the pairs ($\langle p_T \rangle_{\text{pair}}$) is presented in Fig. 1, for a wide range of center-of-mass energies ($\sqrt{s}$) [11].

The values of $\langle p_T \rangle_{\text{pair}}$ are large, and they increase ap-

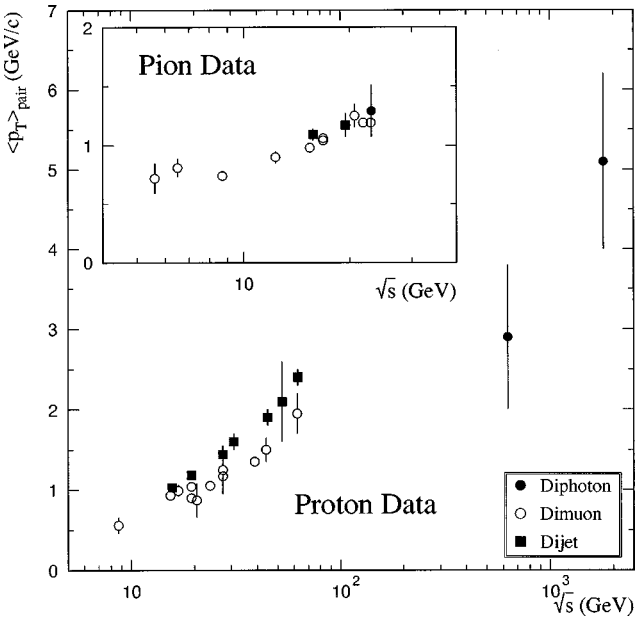

FIG. 1. $\langle p_T \rangle$ of pairs of muons, photons, and jets produced in hadronic collisions versus $\sqrt{s}$.

proximately logarithmically with increasing $\sqrt{s}$. The values of $\langle k_T \rangle$ per parton (estimated as $\approx \langle p_T \rangle_{\rm pair}/\sqrt{2}$) indicated by these DY, diphoton, and dijet data, as well as the inclusive direct-photon and π^0 production data, are too large to be interpreted as ''intrinsic'' — i.e., due only to the finite size of the proton. (From these data, one can infer that the average k_T per parton is about 1 GeV/c at fixed-target energies, increasing to 3–4 GeV/c at the Fermilab Tevatron collider. One would expect $\langle k_T \rangle$ values on the order of 0.3–0.5 GeV/c based solely on proton size.) Perturbative QCD (PQCD) corrections at NLO level are also insufficient to explain the size of the observed effects, and full resummation calculations are required to describe DY and W/Z [12–14], and diphoton [15,16] distributions. Values of $\langle p_T \rangle_{\rm pair}$ for DY and diphoton data exhibit similar trends versus energy; for DY data, pion-beam values are somewhat larger than those for proton beams at the same $\sqrt{s}$. The dijet data hint at somewhat larger values of $\langle p_T \rangle_{\rm pair}$ than DY results at the same energy, a difference that may be related to different color-flow between initial and final states in DY and in dijet events, as well as to a larger contribution from gluon-induced subprocesses for dijet production. Similar soft-gluon (or k_T) effects can be expected to be present in all hard-scattering processes, such as the inclusive production of jets or direct photons [17].

This paper presents a phenomenological model for k_T effects in direct-photon production and, by extension, in all hard-scattering processes. Quantitative comparisons of this model with data from E706 have been reported previously [9,18]. We will discuss the successes and uncertainties of this prescription, as well as the implications for determining the gluon distribution.

k_T SMEARING FORMALISM: THEORY AND PRACTICE

We now briefly describe the theoretical underpinnings of k_T effects using the Collins-Soper-Sterman (CSS) formalism [19]. In this formalism, the p_T spectrum in hard-scattering processes is written as the convolution of the parton distributions $f_{i/h}$, the C functions (representing the finite pieces of the virtual corrections), and two Sudakov form factors, $\mathcal{S}^P$ and $\mathcal{S}^{NP}$. $\mathcal{S}^P$ can be regarded as being perturbative in character and $\mathcal{S}^{NP}$ as non-perturbative. The perturbative Sudakov form factor represents a formal resummation of soft-gluon emissions. The non-perturbative Sudakov form factor is determined from a fit to the data, is expected to be universal (for a given parton flavor and hadron type), and is usually parametrized as a Gaussian distribution. The dividing line between the perturbative and non-perturbative contributions is somewhat arbitrary (similar to the better known cases of parton distributions and fragmentation functions), and it is quantified by a theoretical scale in the resummation formalism. The p_T distribution (e.g., of the Drell-Yan pair) can be written symbolically as

$$\frac{d\sigma}{dp_T} = \sigma_0 e^{-(\mathcal{S}^{NP}+\mathcal{S}^P)} \otimes [(C_{a_1 i} \otimes f_{i/h_1})(C_{a_2 j} \otimes f_{j/h_2})] + Y. \tag{1}$$

The Y function is added to ensure a smooth matching between the low and the high-p_T regions, where the resummed and the fixed-order descriptions work better, respectively.

At collider energies, most of the k_T can be attributed to perturbative soft-gluon emission. However, for fixed-target kinematics, almost all of the k_T is due to the non-perturbative mechanisms. A proper treatment requires both the appropriate data to determine the non-perturbative input, and an implementation of the soft-gluon resummation formalism for the particular process.

The resummation calculation for multiple soft-gluon emission in direct-photon production is quite challenging. The production rate and kinematic distributions of photon pairs produced in hadron interactions have already been calculated [16], and a similar calculation of the transverse momentum distribution of a photon-jet system is also plausible, but more involved, since the final-state parton takes part in soft-gluon emission and in color exchange with the initial-state partons. A recent work on this subject [20] addressed only the effects of multiple soft-gluon radiation in the initial state. Incorporating jet definition in the formalism is also not a fully resolved issue. Finally, the calculation of individual transverse momenta of the photon and the jet is further complicated by the fact that several overlapping power-suppressed corrections can contribute. In the absence of the full resummed calculation, approximations are made in order to compare theory with data.

In lieu of a rigorous calculation of the resummed p_T distribution, effects of soft-gluon radiation can be approximated by a convolution of the leading-order cross section with a k_T-smearing function [21]. In the formalism described above, this is equivalent to absorbing all of the perturbative gluon emissions into the non-perturbative Sudakov form factor. Since no explicit resummation of soft-gluon emissions is performed, the average value of k_T used in the smearing should be representative of the value observed (or expected) in the kinematic regime of the experiment.

The expression for the leading-order (LO) cross section for direct-photon production at large p_T has the form

$$E_\gamma \frac{d^3\sigma}{dp^3}(h_1 h_2 \to \gamma X) = \sum_{a_1 a_2 a_3} \int dx_1 dx_2 f_{a_1/h_1}(x_1, Q^2) f_{a_2/h_2}(x_2, Q^2) \times \frac{\hat{s}}{\pi} \frac{d\sigma}{d\hat{t}}(a_1 a_2 \to \gamma a_3)\, \delta(\hat{s}+\hat{t}+\hat{u}), \tag{2}$$

where $d\sigma/d\hat{t}$ is the hard-scattering parton-level cross section, and f_{a_1/h_1} and f_{a_2/h_2} are the parton distribution functions (pdf) for the colliding partons a_1 and a_2 in hadrons h_1 and h_2, respectively. To introduce k_T degrees of freedom, one extends each integral over the parton distribution functions to the k_T-space,

$$dx_1 f_{a_1/h_1}(x_1, Q^2) \to dx_1 d^2k_{T_1} g(\vec{k}_{T_1}) f_{a_1/h_1}(x_1, Q^2) \tag{3}$$

(a corresponding substitution is done for parton a_2 in hadron h_2).

The distribution $g(\vec{k}_T)$ is usually taken to be a Gaussian,

$$g(\vec{k}_T)=\frac{e^{-k_T^2/\langle k_T^2\rangle}}{\pi\langle k_T^2\rangle}, \tag{4}$$

where $\langle k_T^2\rangle$ is the square of the 2-dimensional (2D) rms width of the k_T distribution for one parton ($\sigma^2_{1\text{parton,2D}}$), and is related to the square of the 2D average of the absolute value of $\vec{k}_T$ of one parton through $\langle k_T^2\rangle=4\langle k_T\rangle^2/\pi$. We emphasize that $\langle k_T\rangle$ represents the average effective 2D transverse momentum per parton. (The average transverse momentum of the parton pair is, of course, a factor of $\sqrt{2}$ larger than the average transverse momentum per parton.)

The 4-vectors of the colliding partons are expressed in terms of the momentum fraction x of the partons. Ignoring parton and hadron masses,

$$x_1=(E_1+p_{l_1})/\sqrt{s}, \tag{5}$$

where the parton four-vector is

$$p_1=(E_1,\vec{k}_{T_1},p_{l_1}), \tag{6}$$

with

$$E_1=\frac{1}{2}\left[x_1\sqrt{s}+\frac{k_{T_1}^2}{x_1\sqrt{s}}\right], \tag{7}$$

and

$$p_{l_1}=\frac{1}{2}\left[x_1\sqrt{s}-\frac{k_{T_1}^2}{x_1\sqrt{s}}\right]. \tag{8}$$

(Similar expressions are used for parton a_2.)

It is straightforward to evaluate the invariant cross sections, including k_T effects, according to the above prescription. In general, because the unmodified PQCD cross sections fall rapidly with increasing p_T, the net effect of k_T smearing is to increase the predicted yield. We denote the enhancement factor as $K(p_T)$. Since the invariant cross section for direct-photon production is now a six-dimensional integral, it is convenient to employ Monte Carlo techniques in the evaluation of $K(p_T)$. An exact treatment of the kinematics can be implemented in a Monte Carlo framework, but it is more difficult in an analytic approach.

A Monte Carlo program that includes such a treatment of k_T smearing, and the leading-order cross section for high-p_T particle production, has long been available [21]. The program provides calculations of many experimental observables, in addition to inclusive cross sections. The program can be used for direct photons, jets, and for single high-p_T particles resulting from jet fragmentation (such as inclusive π^0 production). Unfortunately, no such program is available for NLO calculations, but one can approximate the effect of k_T smearing by multiplying the NLO cross sections by the LO k_T-enhancement factor. Admittedly, this procedure involves a risk of double-counting since some of the k_T-enhancement may already be contained in the NLO calculation. However, we expect such double-counting effects to be small, and consequently this uncertainty on $K(p_T)$ should also be small. (For example, the NLO estimate for $\langle p_T\rangle_{\text{pair}}$ of the diphoton pairs produced in $pp\rightarrow\gamma\gamma$ at $\sqrt{s}=31.5$ GeV is on the order of a few hundred MeV/c, while the resummed prediction is well over 1 GeV/c [14].)

It is clear that this type of treatment of k_T effects is model dependent. In particular, different functional forms can lead to quantitatively different answers. For example, adding substantial non-Gaussian tails in k_T smearing can affect the output distributions. One of the strengths of the approach we follow in this paper is that the k_T distribution used in the smearing is based on experimental information, and the Gaussian character of the k_T effects is consistent with the data observed by E706 [9]. Moreover, any non-Gaussian tails may result primarily from single hard-gluon emission, and such contributions should therefore already be contained in the NLO cross sections used in this analysis.

A complete treatment of soft-gluon radiation in high-p_T production, including the appropriate non-perturbative input, should eventually predict the effective k_T values expected for each process and $\sqrt{s}$. We will employ $\langle k_T\rangle$ values representative of the kinematic distributions in the data, and based on comparisons with the same model as used to modify the NLO inclusive cross sections.

The effects of soft-gluon radiation are also included in QCD Monte Carlo programs such as PYTHIA [22], ISAJET [23], and HERWIG [24]. However, in these programs the emission is normally cut off at a relatively high parton virtuality, with the remaining k_T effect supplied by a Gaussian smearing similar to that discussed above. For fixed-target energies, essentially all of the k_T effects are provided by this phenomenological Gaussian term. The above programs differ in the details of the way parton energy and momentum are rescaled after k_T is inserted, which can also produce quantitative differences in results.

APPLICATIONS OF THE k_T MODEL TO DATA

The experimental consequences of k_T smearing are expected to depend on the collision energy. At the Tevatron collider, the smallest photon p_T values probed by the CDF and D0 experiments are rather large (10–15 GeV/c), and the k_T-enhancement factors modify only the very lowest end of the p_T spectrum, where p_T is not significantly larger than k_T. In the energy range of the E706 measurements, large k_T-effects can modify both the normalizations and the shapes of the cross sections as functions of p_T. Consequently, E706 data provide a particularly sensitive test of the k_T model. At lower fixed-target energies, the k_T enhancements are expected to have less p_T dependence over the range of available measurements, and can therefore be masked more easily by uncertainties in experimental normalizations and/or choices of theoretical scales. Nonetheless, the UA6 and WA70 data generally support expectations from k_T smearing.

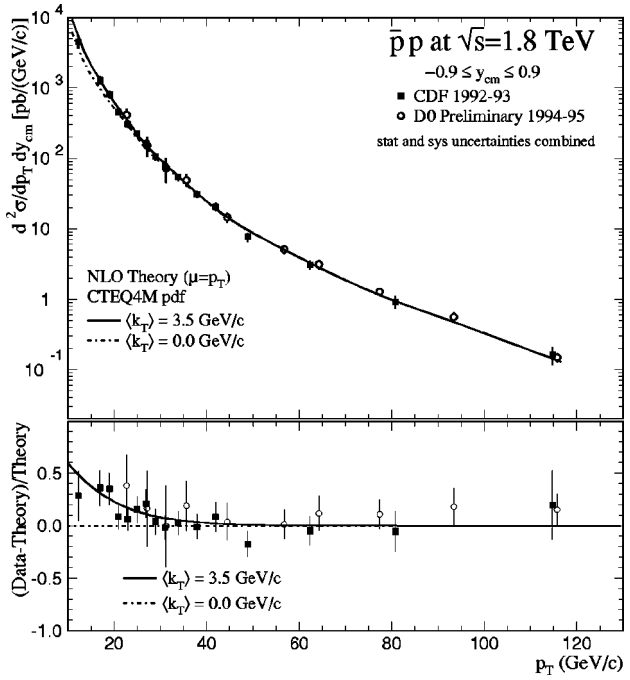

FIG. 2. Top: The CDF and D0 isolated direct-photon cross sections, compared to NLO theory without k_T (dashed) and with k_T enhancement for $\langle k_T\rangle = 3.5$ GeV/c (solid), as a function of p_T. Bottom: The quantity (data−theory)/theory (for theory without k_T adjustment), overlaid with the expected effect from k_T enhancement for $\langle k_T\rangle = 3.5$ GeV/c. The error bars have experimental statistical and systematic uncertainties added in quadrature.

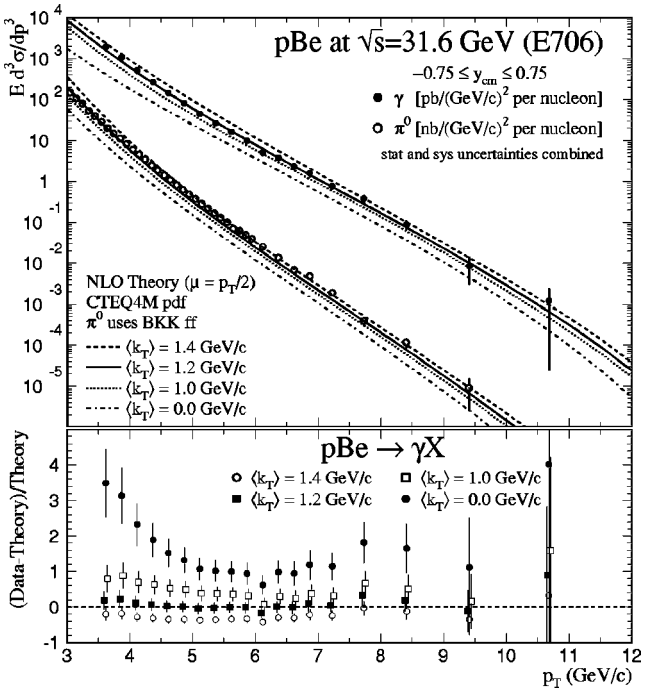

FIG. 3. Top: The photon and π^0 cross sections from E706 at $\sqrt{s}=31.6$ GeV compared to k_T-enhanced NLO calculations. Bottom: The quantity (data−theory)/theory for direct-photon production, using k_T-enhanced NLO calculations for several values of $\langle k_T\rangle$. The error bars have experimental statistical and systematic uncertainties added in quadrature. The points corresponding to calculations with different $\langle k_T\rangle$ are slightly staggered in p_T, to reduce the overlap of experimental error bars.

Comparisons to Tevatron collider data

At the Tevatron collider, the above model of soft-gluon radiation leads to a relatively small modification of the NLO cross section. In Fig. 2 we compare the CDF and D0 isolated direct-photon cross sections [25] to theoretical NLO calculations with and without k_T enhancement. In the lower part of the plot we display the quantity (data−theory)/theory; for the collider regime we did not multiply the NLO theory by the k_T-enhancement factor, but instead displayed the full deviation of the NLO calculation from the data. The expected effect from k_T enhancement is also shown for $\langle k_T\rangle = 3.5$ GeV/c. This is the approximate value of $\langle k_T\rangle$ per parton measured in diphoton production at the Tevatron [25], and one expects a similar $\langle k_T\rangle$ per parton for single-photon production. (In the diphoton process, the 4-vectors of the photons can be measured precisely, providing a direct determination of the transverse momentum of the diphoton system, and thereby $\langle k_T\rangle$.)

As seen in Fig. 2, the k_T effect diminishes rapidly with increasing p_T and is essentially negligible above ≈ 30 GeV/c. The trend of deviations of NLO calculations from the measured inclusive cross sections is described reasonably well by the expected k_T effect. Some of the observed excess can be attributed to the fragmentation contribution to isolated direct-photon production [26], but this alone cannot account for the entire deviation of the theory from data.

The larger statistics in the Tevatron collider run IB samples (currently under analysis) will allow for a more detailed examination of the low-p_T behavior of the photon cross section. (The CDF data included in the plot are from run IA only.) A similar enhancement is expected for jet production at low p_T, but larger experimental uncertainties, and the relatively large additional non-perturbative effects expected in this region [27], preclude a useful comparison.

Comparisons to E706 data

The conventional ($\langle k_T\rangle = 0$) NLO calculations yield cross sections that are signficantly below the E706 direct-photon and π^0 measurements [9] (see Figs. 3, 4, and 5). No choices of current parton distributions, or conventional PQCD scales provide an adequate description of the data (for the comparisons presented here all QCD scales have been set to $p_T/2$). The previously described k_T-enhancement algorithm was used to incorporate the effects of soft-gluon radiation in the calculated yields. That is, the theory results plotted in the figures represent the NLO calculations multiplied by k_T-enhancement factors $K(p_T)$ [28].

Because parton distributions for nucleons are known better than those for pions, we first present comparisons of the various model calculations with proton-beam data. As seen at the bottoms of Figs. 3 and 4, the NLO theory, when supplemented with appropriate k_T enhancements, is successful in describing both the shape and normalization of the E706 direct-photon cross sections at both $\sqrt{s}=31.6$ GeV and 38.8 GeV. As expected, the k_T-enhancement factors af-

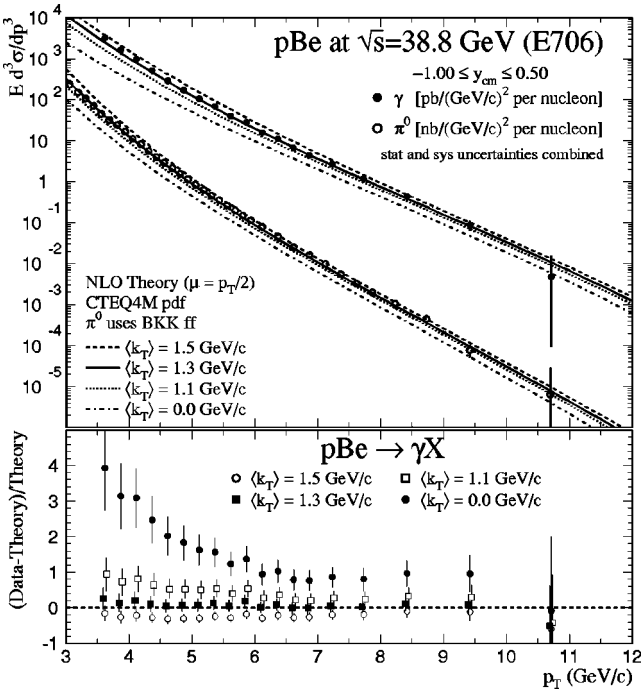

FIG. 4. Top: The photon and π^0 cross sections from E706 at $\sqrt{s}=38.8$ GeV compared to k_T-enhanced NLO calculations. Bottom: The quantity (data−theory)/theory for direct-photon production, using k_T-enhanced NLO calculations for several values of $\langle k_T \rangle$. The error bars have experimental statistical and systematic uncertainties added in quadrature.

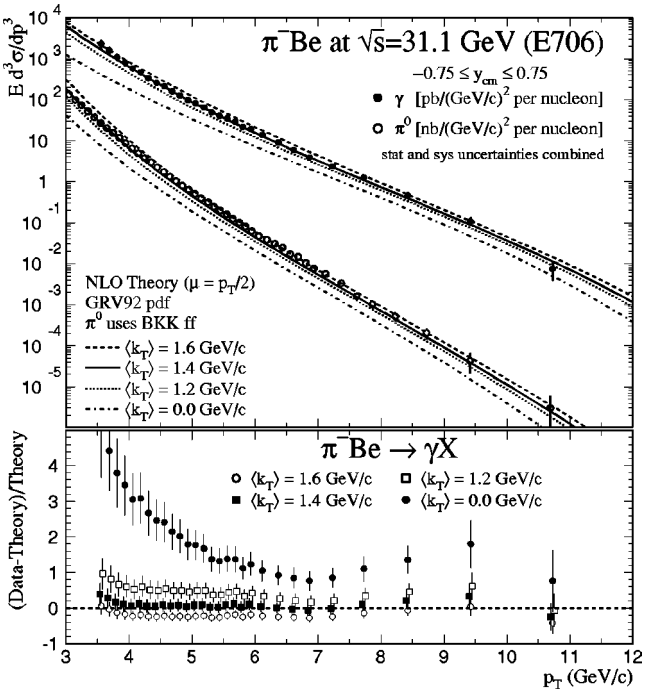

FIG. 5. Top: The photon and π^0 cross sections from E706 at $\sqrt{s}=31.1$ GeV for incident π^- beam, compared to k_T-enhanced NLO calculations. Bottom: The quantity (data−theory)/theory for direct-photon production, using k_T-enhanced NLO calculations for several values of $\langle k_T \rangle$. The error bars have experimental statistical and systematic uncertainties added in quadrature.

fect the normalization of the cross sections, as well as the shapes of the p_T distributions. The values of $\langle k_T \rangle = 1.2$ GeV/c at $\sqrt{s}=31.6$ GeV, and 1.3 GeV/c at $\sqrt{s}=38.8$ GeV, provide good representations of the incident-proton data. Both k_T values are consistent with those emerging from a comparison of the same PQCD Monte Carlo calculations with E706 data on the production of high-mass $\pi^0\pi^0$, $\gamma\pi^0$, and $\gamma\gamma$ pairs [9].

In Fig. 5 we present comparisons between calculations and E706 data for π^-Be interactions at $\sqrt{s}=31.1$ GeV. Here again, the uncorrected ($\langle k_T \rangle = 0$) NLO theory is not consistent with the data. Once the k_T-enhancement factors are applied, good agreement is observed between data and calculations for $\langle k_T \rangle \approx 1.4$ GeV/c. (Note that DY data lead one to expect a higher value of $\langle k_T \rangle$ for a π^- beam than for a proton beam of the same energy.)

For comparison, results of calculations using $\langle k_T \rangle$ values ± 0.2 GeV/c relative to the central values are also shown in the figures. These can be taken as an indication of uncertainties on $\langle k_T \rangle$ (see next section). The corresponding enhancement factors $K(p_T)$ at $\sqrt{s}=31.6$ GeV are displayed in Fig. 6.

It is interesting to note that, in this energy range, the k_T enhancement does not decrease with increasing p_T (as for the case of the collider), and, in fact, increases at the highest values of p_T. This is a consequence of the wide x-range spanned by E706, and can be understood through the following argument. At low p_T, a $\langle k_T \rangle$ of 1.2 GeV/c is non-negligible in comparison to the p_T in the hard-scattering, and the addition of k_T smearing therefore increases the size of the cross section (and steepens the slope in p_T). At highest p_T (corresponding to large x), the unmodified NLO cross section becomes increasingly steep (due to the rapid fall in par-

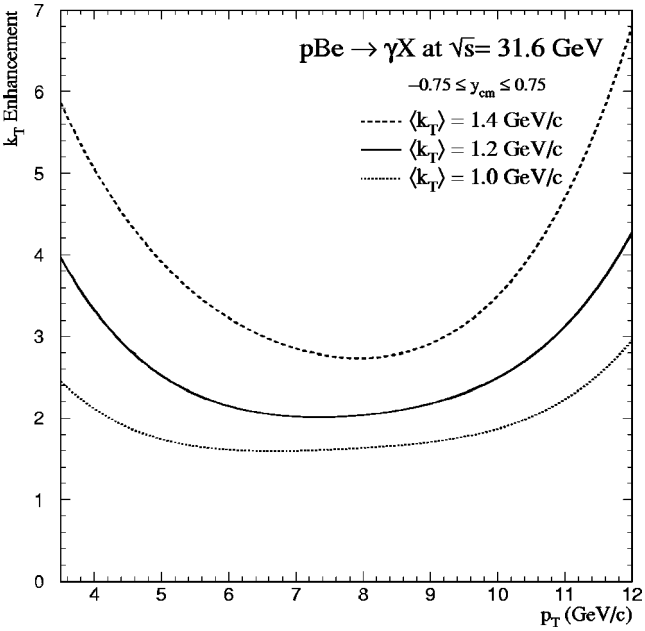

FIG. 6. The variation of k_T enhancements, $K(p_T)$, relevant to the E706 direct-photon data for protons at $\sqrt{s}=31.6$ GeV, for different values of $\langle k_T \rangle$.

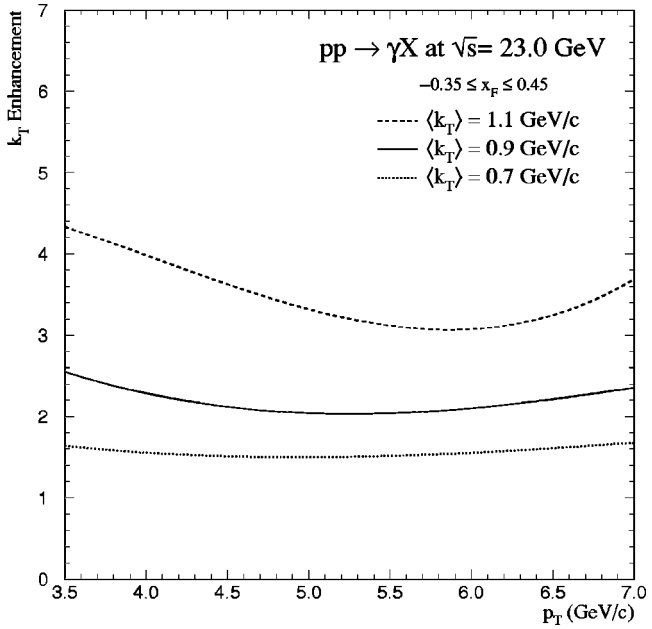

FIG. 7. The k_T-enhancement factors for direct-photon production expected for WA70 pp data.

ton densities), and hence the effect of k_T smearing again becomes larger.

NLO calculations for π^0 production have a greater theoretical uncertainty than those for direct-photon cross sections since they involve parton fragmentation. However, the k_T effects in π^0 production can be expected to be generally similar to those observed in direct-photon production, and the π^0 data can be used to extend tests of the consequences of k_T smearing. Figures 3, 4, and 5 also show comparisons between NLO calculations [29] and π^0 production from E706, using Binnewies-Kniehl-Kramer (BKK) fragmentation functions (ff) [30]. The previously described Monte Carlo program was employed to generate k_T-enhancement factors for π^0 cross sections, and $\langle k_T \rangle$ per parton values similar to those that resulted in good agreement with direct-photon data also provide a reasonable description of π^0 production. For π^0 production, an additional smearing of the transverse momentum, expected from jet fragmentation, has also been taken into account.

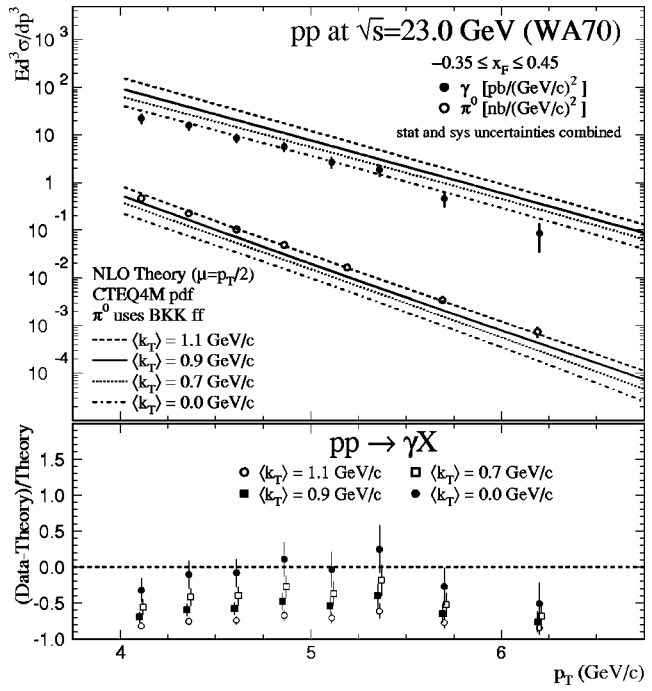

FIG. 8. Top: The photon and π^0 cross sections from WA70 at $\sqrt{s}=23.0$ GeV for incident protons compared to k_T-enhanced NLO calculations. Bottom: The quantity (data−theory)/theory for direct-photon production, using k_T-enhanced NLO calculations for several values of $\langle k_T \rangle$. The error bars have experimental statistical and systematic uncertainties added in quadrature.

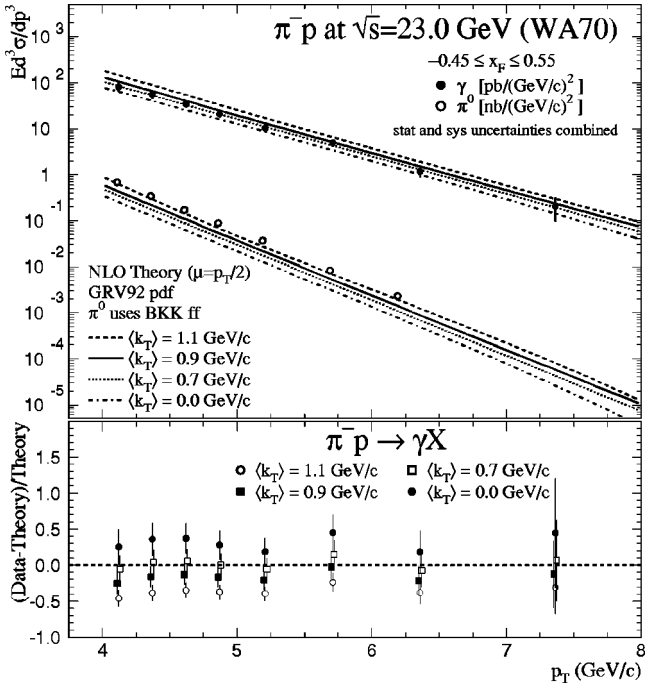

FIG. 9. Top: The photon and π^0 cross sections from WA70 at $\sqrt{s}=23.0$ GeV for incident π^- beam, compared to k_T-enhanced NLO calculations. Bottom: The quantity (data−theory)/theory for direct-photon production, using k_T-enhanced NLO calculations for several values of $\langle k_T \rangle$. The error bars have experimental statistical and systematic uncertainties added in quadrature.

Comparisons to WA70 and UA6 data

We have examined the expectations for the size of soft-gluon effects for fixed-target experiments WA70 and UA6. Both experiments have measured direct-photon production with good statistics, and their data have been included in recent global fits to parton distributions. WA70 measured direct-photon and π^0 production in pp and $\pi^- p$ collisions at $\sqrt{s}=23.0$ GeV [31], and UA6 has recently published [10] their final results (with substantially reduced uncertainties) for direct-photon production in pp and $\overline{p}p$ collisions at $\sqrt{s}=24.3$ GeV. These center of mass energies are somewhat smaller than those of E706, and the $\langle k_T \rangle$ values are therefore expected to be smaller (perhaps of the order of

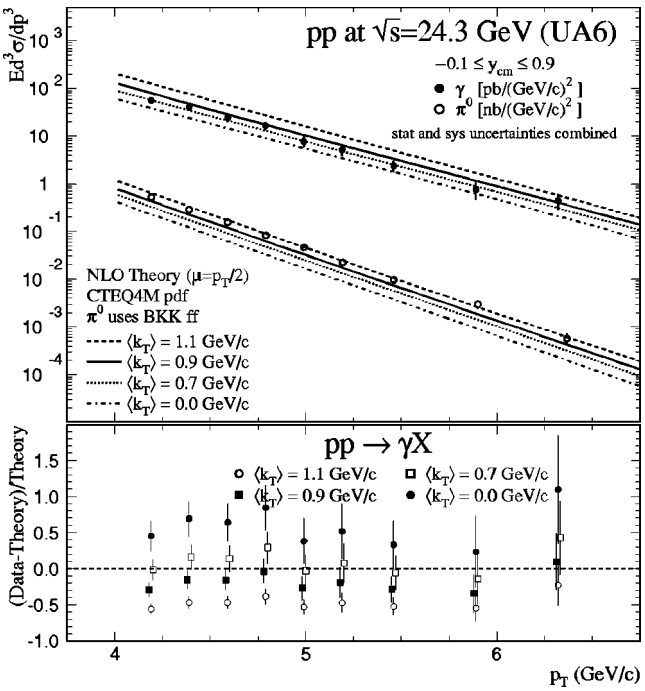

FIG. 10. Top: The photon and π^0 cross sections from UA6 at $\sqrt{s}=24.3$ GeV for an incident proton beam compared to k_T-enhanced NLO calculations. Bottom: The quantity (data–theory)/theory for direct-photon production, using k_T-enhanced NLO calculations for several values of $\langle k_T \rangle$. The error bars have experimental statistical and systematic uncertainties added in quadrature.

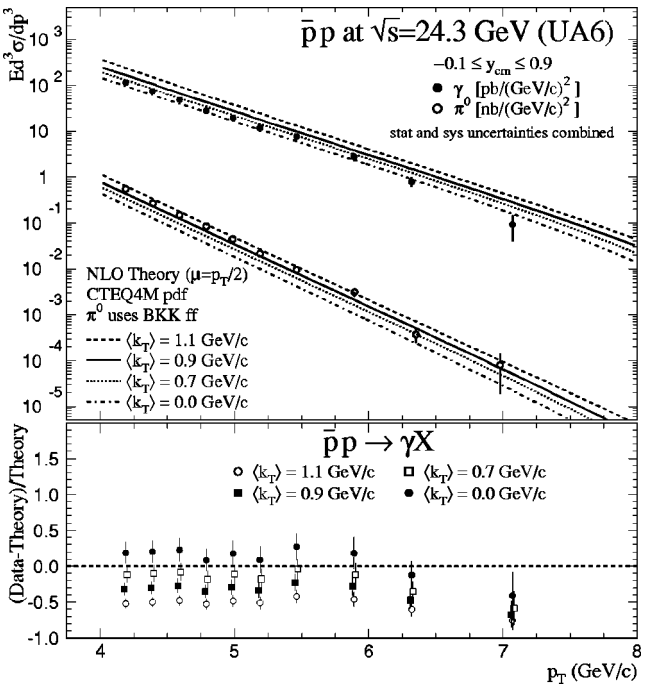

FIG. 11. Top: The photon and π^0 cross sections from UA6 at $\sqrt{s}=24.3$ GeV for an incident antiproton beam compared to k_T-enhanced NLO calculations. Bottom: The quantity (data–theory)/theory for direct-photon production, using k_T-enhanced NLO calculations for several values of $\langle k_T \rangle$. The error bars have experimental statistical and systematic uncertainties added in quadrature.

0.7–0.9 GeV/c, based on Fig. 1). WA70 has compared kinematic distributions observed in diphoton events (for $\pi^- p$ interactions) to NLO predictions, and has found that smearing the NLO theory with an additional $\langle k_T \rangle$ of 0.9 ± 0.2 GeV/c provides agreement with their data [32]. We therefore use this $\langle k_T \rangle$ as the central value for the k_T-enhancement factors for both experiments, and vary the $\langle k_T \rangle$ by ± 0.2 GeV/c, as with E706. The corresponding k_T enhancement expected over the range of measurements is shown in Fig. 7. Over this narrower p_T range, the effect of k_T is essentially to produce a shift in normalization.

Comparisons of the WA70 direct-photon and π^0 cross sections with the k_T-enhanced NLO calculations are shown in Figs. 8 and 9. Renormalization and factorization scales of $p_T/2$ are used in the NLO calculations, as in the E706 comparisons. The π^0 cross sections both for incident proton and π^- beams, and the photon data from incident π^- beam, all lie above the NLO calculations for $\langle k_T \rangle = 0$, and are in better agreement with the k_T-enhanced calculations; only the photon cross section for incident protons seems not to require a k_T correction.

The latest photon cross sections from UA6 for pp and $\bar{p}p$ scattering are shown in Figs. 10 and 11. The photon cross section for pp interactions lies clearly above the NLO calculation for $\langle k_T \rangle = 0$, but is consistent with k_T-adjusted calculations for $\langle k_T \rangle$ in the range of 0.7–0.9 GeV/c. The result for $\bar{p}p$ interactions is also above the unmodified NLO calculation, but requires a smaller value of $\langle k_T \rangle$. We note that the dominant production mechanisms for the two processes are different: quark-gluon Compton scattering dominates for pp, and $\bar{q}q$ annihilation for $\bar{p}p$ at the UA6 energy. As in the case of E706 and WA70 measurements, the UA6 π^0 cross sections are also higher than the NLO calculation without k_T, and can be much better described by introducing k_T enhancement.

DISCUSSION OF k_T-SMEARING PROCEDURES

In this section, we consider uncertainties in the Monte Carlo method employed in our previous discussion, and comment on an analytic approach for calculating such k_T enhancements.

Uncertainties in the Monte Carlo model and related issues

Our approach contains several phenomenological parameters that affect the range of its results, the most important of which is the amount of Gaussian smearing represented by $\langle k_T \rangle$. Thus far, both the value of $\langle k_T \rangle$ (with its dependence on $\sqrt{s}$) and its possible range of uncertainty can only be determined empirically. A range of variation of ± 0.2 GeV/c for $\langle k_T \rangle \sim 1$–2 GeV/$c$ appears reasonable on the basis of several considerations. These include: (i) the range of k_T values inferred from high-mass pair distributions in E706 data; (ii) observed differences between photon and π^0 results; (iii) comparisons of $\langle k_T \rangle$ values required in in-

clusive cross sections to those representing the properties of massive pairs at E706 and WA70/UA6 energies, and (iv) differences between dimuon, diphoton, and dijet values of $\langle p_T \rangle_{\rm pair}$ seen in Fig. 1. (The dependence of the k_T-enhancement factor on the variation in $\langle k_T \rangle$ was illustrated in Figs. 6 and 7.)

For the fixed-target experiments discussed in the previous section, we already presented calculations using $\langle k_T \rangle$ values of 0.2 GeV/c above and below the selected central values. The observed variation in predictions reflects an uncertainty in the k_T-enhanced theoretical results. The dependence of $K(p_T)$ on $\langle k_T \rangle$ is especially strong at the extremes (low and high) in p_T. These calculations used renormalization and factorization scales of $p_T/2$. Changing the scale to p_T reduces predicted cross sections at fixed-target energies by about 30–40 %, a factor comparable to the estimated spread in the k_T factors over much of the p_T range; the full uncertainty in the calculations must include contributions from uncertainties in both $\langle k_T \rangle$ and QCD scales.

Another parameter in the model, a propagator mass m, is introduced to regularize the divergences of the leading-order QCD matrix elements due to the propagator factors $1/\hat{s}$, $1/\hat{t}$, and $1/\hat{u}$ in the configuration where one or more of these invariants approaches zero. To avoid the large weights associated with these configurations, the propagators are replaced by $1/(\hat{s}+m^2)$, $1/(\hat{t}-m^2)$, and $1/(\hat{u}-m^2)$, respectively, where m has a typical value of order 1 GeV. The physical effect of the propagator mass is to cut off the region where almost all of the transverse momentum of the produced photon is due to the Gaussian smearing, and very little to the hard scattering. While the k_T-enhancement factor is relatively insensitive to the value of m for the measured range at collider energies, it is somewhat sensitive for data at fixed-target energies.

To illustrate the sensitivity of the k_T-enhancement factor $K(p_T)$ to the choice of the propagator mass, we display in Fig. 12 the results for $m=1.0$ GeV (default value), 1.3 GeV, and 0, for $p\mathrm{Be}\rightarrow\gamma X$ at $\sqrt{s}=31.6$ GeV. Above p_T values of 5.5–6.0 GeV/c, the k_T enhancement has little sensitivity to m. At lower p_T, the dependence on the propagator mass should be considered as a measure of an uncertainty of the model in this region of phase space. Clearly, larger enhancements are obtained at low p_T when there is no propagator mass ($m=0$).

The value of $\langle k_T \rangle$, appropriate in the calculation, depends on the kinematic situation. The increase of the value of $\langle k_T \rangle$ with s is understood, in general terms, as the result of an increase in the available phase space for multiple-soft-gluon emission. This growth is predicted by a CSS-type of resummation for Drell-Yan processes [33] and, as illustrated in Fig. 1, has been observed in Drell-Yan and diphoton data. For simplicity, the model calculation assumes a constant value of $\langle k_T \rangle$ for a given $\sqrt{s}$. In reality, various physical effects can modify this simple choice and cause a modification in the shape of the enhancement factor $K(p_T)$. Below, we discuss a few of these effects.

First, one might expect a dependence of $\langle k_T \rangle$ on $\hat{s}$, the hardness of the partonic interaction, similar to that on s. A

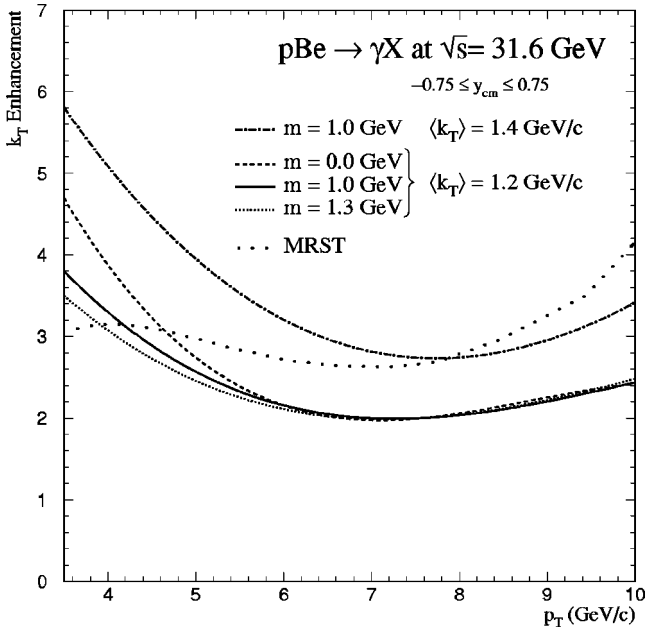

FIG. 12. The effect of different propagator masses m for predictions of k_T enhancements $K(p_T)$ for E706 direct-photon data at $\sqrt{s}=31.6$ GeV. The k_T enhancement used by the MRST group [36] is also shown in the figure.

study of diphoton production at $\sqrt{s}=31.5$ GeV, using the RESBOS program [14], indicates that the $\langle k_T \rangle$ increases from about 1.2 GeV/c for photons with p_T of 5 GeV/c to approximately 1.4 GeV/c for photons with p_T of 10 GeV/c. If direct-photon production were to have a similar behavior, the anticipated k_T enhancement at a p_T of 10 GeV/c would be about 40% higher than for a constant $\langle k_T \rangle$ value of 1.2 GeV/c (see the dependence of the enhancement factor on $\langle k_T \rangle$ in Fig. 6).

Suppression mechanisms may also exist at large p_T due to the restriction of phase space for gluon emission from large-x partons. A gluon emitted from an incoming parton carries away a momentum fraction $\Delta x=2p_T e^y/\sqrt{s}$, where y is the rapidity of the gluon. Since gluons emitted at forward rapidities would carry away more of the incident parton's momentum than available, the effective rapidity range for gluon emission becomes restricted to central rapidities. Such effects are not taken into account correctly in the simple k_T models discussed above.

Finally, there has been much recent interest in studying the effects of resumming large logarithms of the form $\ln(1-x_T)$, where $x_T=2p_T/\sqrt{s}$ [34,35]. As x_T approaches 1, for any hard-scattering process, the perturbative cross section is enhanced by powers of $\ln(1-x_T)$ that have to be resummed at all orders. These types of effects should currently be negligible for direct-photon production at the Tevatron collider (because data are available only for relatively small values of x_T), but may be important at fixed-target energies. Definitive answers to the question of whether this effect leads to a net enhancement or suppression, and its consequences for the shape of the p_T distribution, are not presently available. A treatment that includes both k_T and threshold resummation

effects may be necessary for a more satisfactory description of the fixed-target data.

Analytic smearing methods

An alternative to the Monte Carlo calculation of the k_T enhancement is its implementation through analytic convolution of the theoretical cross section with a (Gaussian) k_T distribution in either one or two dimensions. The latter is a better approximation, but the correction to the one-dimensional convolution is second order in k_T/p_T, leading to a difference of about 10% for the fixed-target applications. To compare to the Monte Carlo results, the parameters of such analytic convolutions must be interpreted in terms of the parton-level $\langle k_T \rangle$ values.

We consider the kinematics of the production of a direct photon accompanied by a recoil jet. As mentioned before, the total transverse momentum imparted to the final state (γ+jet) by the colliding partons has an rms width

$$\sigma_{2\text{partons,2D}} = \sqrt{2}\,\sigma_{1\text{parton,2D}}. \tag{9}$$

However, the single photon is subject only to half of this transverse kick, because it shares the total p_T with the recoil jet. Consequently, the k_T rms width relevant for an analytic smearing of the single-inclusive photon cross section is

$$\sigma_{\gamma,\text{2D}} = \frac{1}{2}\sigma_{2\text{parton,2D}} = \frac{1}{\sqrt{2}}\sigma_{1\text{parton,2D}}. \tag{10}$$

The above can be illustrated by a simple example. Consider the production of a photon and a jet with equal and opposite p_T values (for example, 4 GeV/c) close to 90 degrees in the center of mass. Compare this to the situation when the colliding partons impart some amount of k_T, say 1 GeV/c, in the direction of the photon. The photon p_T is now 4.5 GeV/c, and the jet p_T becomes 3.5 GeV/c (in the opposite direction), resulting from a total of 1 GeV/c of k_T imparted to the photon+jet system. Thus, the photon itself only receives half of the partonic total. This factor of two is critical, and can be easily overlooked, in calculating k_T smearing using analytic methods. The above conclusions have been verified within the explicit Monte Carlo treatment of event kinematics. (The convolution formulas for k_T smearing are discussed more fully in the Appendix.)

Recently, the MRST group has produced a new set of parton distributions, incorporating k_T effects in their analysis of the WA70 and E706 direct-photon data [36]; they used an analytic smearing technique rather than a Monte Carlo approach. The correction algorithm differs in detail with the one discussed above, and seems to require a significantly smaller $\langle k_T \rangle$ to describe the data (about 0.65 GeV/c per incoming parton as compared to 1.2 GeV/c that was used for E706 at $\sqrt{s}=31.6$ GeV). This discrepancy may be due to a difference in the interpretation of k_T that is related to the factor of two present in Eq. (10). If we reinterpret the MRST value of 0.65 GeV/c as our 1.3 GeV/c per parton, then agreement is restored. Nevertheless, the k_T-enhancement factors differ somewhat in the two techniques, leading to different conclusions about the gluon distribution, especially at large x (see next section). For comparison, the MRST k_T factor for E706 (at $\sqrt{s}=31.6$ GeV) has also been plotted in Fig. 12; it is similar in size to our calculations for $\langle k_T \rangle$ values in the range of 1.2–1.4 GeV/c, but has a different shape in p_T. Until these differences are understood, we must assume that there is a significant shape-dependent uncertainty associated with the particular assumptions used for modeling k_T effects.

IMPACT ON THE GLUON DISTRIBUTION

It is now generally accepted that the uncertainty in the gluon distribution at large x is still quite large. Thus, it would appear important to incorporate further constraints on the gluon, especially from direct-photon data. In the following, we describe a global pdf fit that employs our k_T model in the analysis of E706 direct-photon measurements. Since jet production at the Tevatron collider is another available constraint for the gluon content at large x, we discuss the consistency between the E706 direct-photon results and the CTEQ4HJ gluon distribution (derived using high-p_T jet data from CDF) [37].

Application of k_T enhancements in a pdf fit

To investigate the impact of k_T effects on determinations of the gluon distribution, we have included the E706 direct-photon cross sections for incident protons, along with the DIS and DY data that were used in determining the CTEQ4M pdfs, in a global fit to the parton distribution functions. The CTEQ fitting program was employed to obtain these results [38], using the NLO PQCD calculations for direct-photon cross sections, adjusted by the k_T-enhancement factors. However, the WA70, UA6, CDF, and D0 data were excluded from this particular fit. The resulting gluon distribution, shown in Fig. 13, is similar to CTEQ4M, as might have been expected, since the k_T-enhanced NLO cross sections using CTEQ4M provide a reasonable description of the data shown in Figs. 3 and 4.

The data sets used in determining CTEQ4M did not include the E706 direct-photon cross sections, but did use earlier direct-photon data from UA6 and from WA70 (without k_T corrections), along with the inclusive jet cross sections from CDF and D0 [39]. The jet cross sections were particularly useful for defining the gluon distribution in CTEQ4M at moderate values of x.

The new MRST gluon distribution (also shown in Fig. 13) is significantly lower than CTEQ4M (and MRSR2) at large x. While the MRST fit employs k_T enhancements, it attempts to accommodate the WA70 incident-proton direct-photon data, which does not exhibit an obvious k_T effect. In addition, the MRST k_T-enhancement factors are larger at large p_T than our corresponding results, resulting in a smaller gluon at large x. This further serves to illustrate the extent to which the extracted gluon distribution is affected by the specific procedures applied in the fit. In contrast, the CTEQ4HJ specialized gluon distribution (discussed in more detail in the next subsection) is much larger than CTEQ4M in the same x

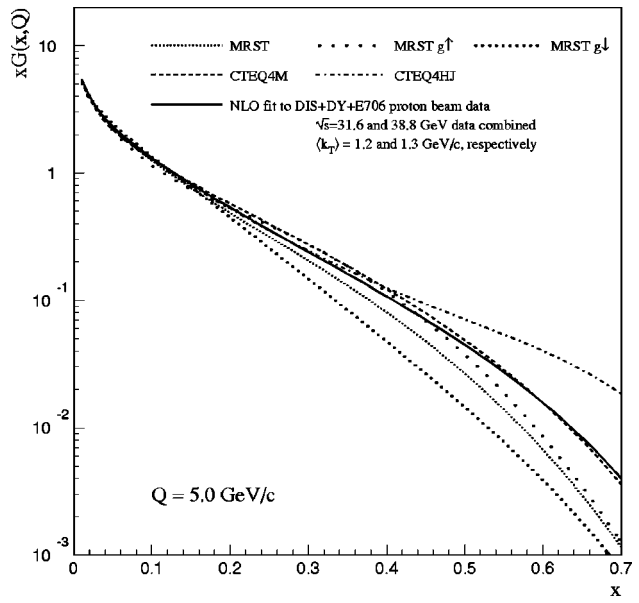

FIG. 13. A comparison of the CTEQ4M, MRST, and CTEQ4HJ gluons, and the gluon distribution derived from fits that use E706 data. The $g\uparrow$ and $g\downarrow$ gluon densities correspond to the maximum variation in $\langle k_T \rangle$ that MRST allowed in their fits.

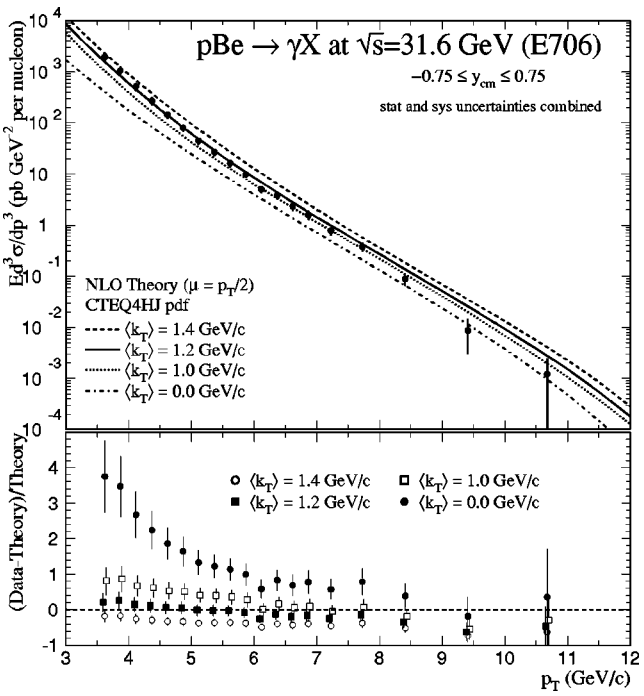

FIG. 14. Top: The photon cross section from E706 at $\sqrt{s}=31.6$ GeV compared to k_T-enhanced NLO calculations using the CTEQ4HJ parton distribution functions. Bottom: The quantity (data−theory)/theory using k_T-enhanced NLO calculations for several values of $\langle k_T \rangle$. The error bars have experimental statistical and systematic uncertainties added in quadrature.

range. The current spread of the solutions for the gluon distribution at large x is uncomfortably large, and additional theoretical effort is warranted to properly incorporate the available direct-photon data into the pdf fits.

Discussion of the CTEQ4HJ gluon

As presented above, when analyzed with k_T-enhancement factors, the E706 direct-photon data lead to a gluon distribution similar to that in CTEQ4M. The implications for the size of the gluon at large x are especially important because of the excess observed by CDF in the high-p_T inclusive jet cross section (when compared to calculations using conventional pdfs). The CTEQ Collaboration produced a global fit (CTEQ4HJ) [37] to improve the description of the high-p_T jet data from CDF in run IA [40]. The high-p_T data points were given an enhanced weight to emphasize them in that fit. The resulting CTEQ4HJ parton distributions produce a jet cross section that by design follows the CDF data points more closely than the cross section obtained using CTEQ4M.

The CDF inclusive jet cross section from run IB [41] demonstrates an excess at high p_T similar to that observed in run IA. For D0, the inclusive jet cross section from run IA+IB is consistent with the NLO QCD calculation using conventional parton distributions such as CTEQ4M, but can also be well-described with calculations using the CTEQ4HJ parton distribution functions; in fact, calculations using CTEQ4HJ result in better χ^2 agreement with the D0 jet data [42].

The CTEQ4HJ quark distributions are similar to those obtained in a more standard fit (as for example CTEQ4M), since the DIS and DY data provide significant constraints on the quark distributions over all x (and on the gluon distribution at small x) [3]. However, the CTEQ4HJ gluon distribution is significantly larger at high x than that of CTEQ4M, by a factor of 1.5 at $x=0.5$ (for $Q=5$ GeV/c), and by a factor of 5 at $x=0.7$.

Because of the dominance of the $q\bar{q}$ scattering subprocess in the Tevatron jet cross sections at high p_T, a large change in the gluon distribution is required to generate a relatively small change in the jet cross section. As the CTEQ exercise has demonstrated, until the theoretical issues related to interpretation of direct-photon data are resolved, there is freedom within the data sets used in the global fits to change the gluon distribution in this way. It should also be noted that a recent analysis [43] of deuteron and proton structure functions, using corrections for nuclear binding effects in the deuteron, suggests that the down-quark distribution in the nucleon at large x may be significantly larger than previously assumed; clearly this also influences the calculated cross sections for the high-p_T jet production.

The CTEQ4HJ gluon distribution is compared to those from CTEQ4M, MRST, and the fits including the E706 data in Fig. 13. Figures 14 and 15 show comparisons of the E706 direct-photon cross sections and the NLO calculations using the CTEQ4HJ parton distributions, with and without the k_T-enhancement factor. The shape in p_T of these calculations appears less consistent with the data than the corresponding results using the CTEQ4M gluon. However, current uncertainties in the understanding of k_T effects in direct-photon production (discussed in the previous section), preclude an unambiguous interpretation of this difference.

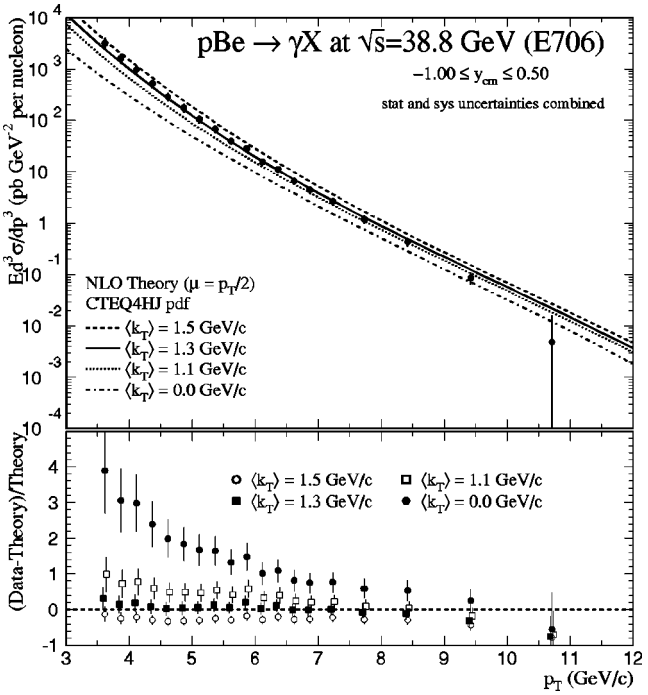

FIG. 15. Top: The photon cross section from E706 at $\sqrt{s}=38.8$ GeV compared to k_T-enhanced NLO calculations using the CTEQ4HJ parton distribution functions. Bottom: The quantity (data−theory)/theory using k_T-enhanced NLO calculations for several values of $\langle k_T\rangle$. The error bars have experimental statistical and systematic uncertainties added in quadrature.

CONCLUSIONS

We have described a phenomenological model for k_T effects in high-p_T inclusive cross sections in which $\langle k_T\rangle$ values used in the calculations of k_T-enhancement factors are derived from kinematic distributions in the high-mass pair data. Despite uncertainties, the results are remarkably successful in reconciling the data and theoretical calculations for a broad range of energies. The k_T-enhancement factors improve the agreement of PQCD calculations with E706, UA6, and π^- beam WA70 direct-photon cross sections over the full p_T range of measurements, and at the low-p_T end of CDF and D0 results. All fixed-target π^0 measurements also agree much better with such k_T-enhanced calculations.

The proper treatment of soft-gluon radiation in direct-photon cross sections can affect the extraction of the gluon distribution, especially at large values of x. In this particular treatment of k_T enhancement, the E706 data, which span the widest x-range of any direct-photon experiment, are in better agreement with the gluon distribution from CTEQ4M than from CTEQ4HJ. However, within the phenomenological approach, any physical mechanism which gives rise to less enhancement at large x than our specific model calculation can make the CTEQ4HJ gluon more consistent with the E706 data.

A definitive conclusion regarding the quantitative role of k_T effects in hard scattering, and reliable additional information on the large-x gluon distribution, awaits more complete theoretical calculations. The new generation of direct-photon and inclusive jet measurements serves as a strong impetus, and provides a testing ground, for new theoretical developments, perhaps incorporating both k_T and large-x resummation, which will have less model dependence than the formulations discussed in this paper. Further progress built on this interplay between theory and experiment will allow a more definitive determination of the gluon distribution, especially in the large-x region, where significant uncertainties still remain.

ACKNOWLEDGMENTS

We thank S. Catani, S. Ellis, E. Kovacs, H.-L. Lai, M. Mangano, P. Nason, T. Sjöstrand, G. Snow, D. Soper, G. Sterman, J. Stirling, M. Werlen, and C.-P. Yuan for useful conversations.

APPENDIX

In this appendix, we collect formulas relevant to the analytic treatment of k_T effects in inclusive cross sections. As discussed in the main text, we assume a Gaussian description for the parton k_T-distributions; the width parameters entering the formulas are labeled explicitly to help keep track of their meaning.

For definiteness, let us consider direct-photon production. The full 2-dimensional convolution of the (parametrized) differential cross section Σ (for example, $\Sigma = d\sigma/dp_T$) with the Gaussian k_T-smearing functions can be written as

$$\Sigma'(p_T) = \int d^2k_{T_1} d^2k_{T_2} d^2q_T \, \frac{1}{\pi\langle k_{T_1}^2\rangle} \times e^{-k_{T_1}^2/\langle k_{T_1}^2\rangle} \frac{1}{\pi\langle k_{T_2}^2\rangle} e^{-k_{T_2}^2/\langle k_{T_2}^2\rangle} \, \Sigma(q_T) \times \delta^{(2)}\left(\vec{p}_T - \vec{q}_T - \frac{1}{2}(\vec{k}_{T_1} + \vec{k}_{T_2})\right), \tag{A1}$$

or, integrating out the δ-function constraints, as

$$\Sigma'(p_T) = \int d^2k_T \frac{1}{\pi\sigma_{\gamma,2\mathrm{D}}^2} \exp(-k_T^2/\sigma_{\gamma,2\mathrm{D}}^2)\Sigma(|\vec{p}_T - \vec{k}_T|), \tag{A2}$$

where $\sigma_{\gamma,2\mathrm{D}}$ is the width parameter appropriate for the smearing of the direct-photon inclusive distribution; it is related to the width of the parton k_T-distribution through Eq. (10).

The k_T-enhancement factors, defined as $K(p_T) \equiv \Sigma'(p_T)/\Sigma(p_T)$, can be calculated numerically. For a more intuitive treatment, one can simplify the discussion by reducing the above equation to a 1-dimensional case. Let us decompose the $\vec{k}_T$ vector into components parallel and perpendicular to $\vec{p}_T$. Then only the parallel component strongly affects the value of the photon p_T, while the perpendicular component affects p_T much less for typical $k_T \ll p_T$ configurations (since it adds to p_T in quadrature). Neglecting the

effect of the perpendicular component, and integrating it out, one arrives at a 1-dimensional approximation:

$$\Sigma'(p_T) = \int_{-\infty}^{+\infty} dk_T \frac{1}{\sqrt{2\pi\sigma_{\gamma,1D}^2}} \exp(-k_T^2/2\sigma_{\gamma,1D}^2)\Sigma(p_T - k_T), \tag{A3}$$

where

$$\sigma_{\gamma,1D} = \frac{1}{\sqrt{2}}\sigma_{\gamma,2D} = \frac{1}{2}\sigma_{1\text{parton},2D}, \tag{A4}$$

and we used Eq. (10) to relate $\sigma_{\gamma,2D}$ and $\sigma_{1\text{parton},2D}$.

Two particularly interesting special cases are the exponential form of the cross section, used to describe the data at fixed-target energies, and the $1/p_T^n$ form, appropriate at colliders.

For an exponential representation of the cross section, $\Sigma \sim \exp(-bp_T)$, one obtains

$$K(p_T) = \exp\left(\frac{1}{8}b^2\sigma_{1\text{parton},2D}^2\right) = \exp\left(\frac{1}{2\pi}b^2\langle k_T\rangle^2\right). \tag{A5}$$

Using the LO calculation of $pp \to \gamma X$ at $\sqrt{s} = 31.6$ GeV (and $\langle k_T\rangle = 0$), one finds $b \approx 1.8$ $(\text{GeV}/c)^{-2}$ at $p_T = 6.5$ GeV/c (a value in the middle of the p_T range of E706). The approximate 1-dimensional formula above yields $K \approx 2.1$ for $\langle k_T\rangle = 1.2$ GeV/c, compared to $K^{\text{LO}} \approx 2.0$ obtained in the full LO Monte Carlo calculation. In general, despite the approximations in the treatment, the analytical results are quite close to the results of the LO calculations. The $1/\sqrt{2}$ factor in the relation of $\sigma_{\gamma,2D}$ and $\sigma_{1\text{parton},2D}$ [Eq. (10)] is crucial to obtaining this consistency.

A different representation, useful, for example, for parametrizing CDF and D0 measurements, assumes $\Sigma \sim 1/p_T^n$. For this parametrization (or more general functional forms) one can expand $\Sigma(p_T - k_T)$ as a power series in k_T (for k_T small compared to p_T):

$$\Sigma(p_T - k_T) = \Sigma(p_T) + \frac{1}{2!}k_T^2\Sigma''(p_T) + \frac{1}{4!}k_T^4\Sigma^{(4)}(p_T) + \cdots \tag{A6}$$

(the odd powers of k_T integrate out to zero). One obtains

$$K(p_T) = 1 + \frac{\langle k_T\rangle^2}{2\pi}\frac{n(n+1)}{p_T^2} + \frac{\langle k_T\rangle^4}{8\pi^2}\frac{n(n+1)(n+2)(n+3)}{p_T^4} + \cdots. \tag{A7}$$

For a constant (or a slowly changing) slope parameter n (and for $\langle k_T\rangle \ll p_T$), the effects of k_T smearing decrease as $1/p_T^2$, as might be expected for a power-suppressed process.

[1] F. Halzen and D. Scott, Phys. Rev. D **21**, 1320 (1980).
[2] P. Aurenche *et al.*, Phys. Lett. **140B**, 87 (1984); Nucl. Phys. **B297**, 661 (1988).
[3] J. Huston *et al.*, Phys. Rev. D **58**, 114034 (1998).
[4] A. Martin, W. Stirling, and R. Roberts, Phys. Lett. B **304**, 155 (1995).
[5] H.L. Lai, Phys. Rev. D **55**, 1280 (1997).
[6] P. Aurenche *et al.*, Phys. Rev. D **39**, 3275 (1989).
[7] M. Glück, E. Reya, and A. Vogt, Z. Phys. C **67**, 433 (1995); **53**, 127 (1992).
[8] J. Huston *et al.*, Phys. Rev. D **51**, 6139 (1995).
[9] L. Apanasevich *et al.*, Phys. Rev. Lett. **81**, 2642 (1998).
[10] G. Ballocchi *et al.*, Phys. Lett. B **436**, 222 (1998).
[11] M. Begel, Ph.D. thesis, University of Rochester, 1998, and references therein.
[12] G. Altarelli, R.K. Ellis, M. Greco, and G. Martinelli, Nucl. Phys. **B246**, 12 (1984).
[13] C. Balázs, C.-P. Yuan, and J.-W. Qiu, Phys. Lett. B **355**, 548 (1995).
[14] C. Balázs and C.-P. Yuan, Phys. Rev. D **56**, 5558 (1997), and references therein.
[15] P. Chiappetta, R. Fergani, and J.Ph. Guillet, Phys. Lett. B **348**, 646 (1995).
[16] C. Balázs, E. Berger, S. Mrenna, and C.-P. Yuan, Phys. Rev. D **57**, 6934 (1998).
[17] R. Feynman, R. Field, and G. Fox, Phys. Rev. D **18**, 3320 (1978); A.P. Contogouris *et al.*, Nucl. Phys. **B179**, 461 (1981); Phys. Rev. D **32**, 1134 (1985); M. Fontannaz and D. Schiff, Nucl. Phys. **B132**, 457 (1978).
[18] G. Altarelli, hep-ph/9710434 (talk at Lepton-Photon '97); H. Montgomery, FERMILAB-CONF-97-193 (talk at DIS '97); M. Zieliński, Nucl. Phys. B (Proc. Suppl.) **64**, 84 (1998) (talk at QCD '97); J. Huston, plenary talk at the ICHEP conference in Vancouver, 1998.
[19] J. Collins and D. Soper, Nucl. Phys. **B193**, 381 (1981); **B213**, 545(E) (1983); **B197**, 446 (1982); J. Collins, D. Soper, and G. Sterman, Phys. Lett. **109B**, 388 (1982); **126B**, 275 (1983); Nucl. Phys. **B223**, 381 (1983); **B250**, 199 (1985).
[20] H.-L. Lai and H.-N. Li, Phys. Rev. D **58**, 114020 (1998).
[21] J. Owens, Rev. Mod. Phys. **59**, 465 (1987).
[22] T. Sjöstrand, hep-ph/9508391.
[23] F. Paige *et al.*, hep-ph/9804321.
[24] G. Marchesini *et al.*, hep-ph/9607393.
[25] See, e.g., S. Linn at the ICHEP conference in Vancouver, 1998.
[26] L.E. Gordon, Nucl. Phys. **B501**, 175 (1997).
[27] S. Ellis, J. Huston, and D. Soper (in preparation).
[28] For E706, each QCD calculation has been adjusted by $A^{\alpha-1}$ to account for nuclear dependence of production on a Be target ($A = 9.01$), using $\alpha = 1.04(1.08)$ for direct-photon (π^0) data.
[29] F. Aversa *et al.*, Nucl. Phys. **B237**, 105 (1989).
[30] J. Binnewies, B.A. Kniehl, and G. Kramer, Phys. Rev. D **52**, 4947 (1995).
[31] M. Bonesini *et al.*, Z. Phys. C **38**, 371 (1988); **37**, 535 (1988); **37**, 39 (1987).

[32] E. Bonvin *et al.*, Phys. Lett. B **236**, 523 (1990); Z. Phys. C **41**, 591 (1989).
[33] See, e.g., W.J. Stirling and M.R. Whalley, J. Phys. G **19**, D1 (1993).
[34] S. Catani, M. Mangano, and P. Nason, J. High Energy Phys. **07**, 024 (1998).
[35] E. Laenen, G. Oderda, and G. Sterman, Phys. Lett. B **438**, 173 (1998); N. Kidonakis, G. Oderda, and G. Sterman, *ibid.* **531**, 365 (1998); Nucl. Phys. **B525**, 299 (1998).
[36] A. Martin, R.G. Roberts, W.J. Stirling, and R.S. Thorne, Eur. Phys. J. C **4**, 463 (1998). In their k_T algorithm, the MRST group smears the perturbative QCD distribution by first making an analytic continuation of $(d\sigma/dp_T^2)_{\mathrm{PQCD}}$ to small p_T (<3 GeV/c) and then convoluting with a Gaussian form $(1/\pi\sigma)e^{-k_T^2/\sigma}$, where $\sigma=(4/\pi)\langle k_T\rangle^2_{\mathrm{MRST}}$.
[37] J. Huston *et al.*, Phys. Rev. Lett. **77**, 444 (1996).
[38] H.-L. Lai, Ph.D. thesis, Michigan State University, 1997.
[39] F. Abe *et al.*, Phys. Rev. Lett. **77**, 438 (1996); D. Elvira, at Conference on DIS and Related Phenomena, Rome, 1996.
[40] F. Abe *et al.*, Phys. Rev. Lett. **77**, 438 (1996).
[41] See, e.g., A. Akopian at the Physics in Collision conference, Frascati, 1998.
[42] See, e.g., J. Blazey at the ICHEP conference in Vancouver, 1998.
[43] U.K. Yang and A. Bodek, hep-ph/9806458; U.K. Yang, A. Bodek, and Q. Fan, hep-ph/9806457.